

# **SiO<sub>2</sub> Passivation Layer Grown by Liquid Phase Deposition for N-type Bifacial Silicon Solar Cells**

Y. L. CHEN<sup>1,a</sup>, G. L. LU<sup>1,b</sup>, S. H. ZHONG<sup>1,c</sup> and W. Z. SHEN<sup>1,d\*</sup>

<sup>1</sup>Institute of Solar Energy, and Key Laboratory of Artificial Structures and Quantum Control (Ministry of Education), Department of Physics and Astronomy, Shanghai Jiao Tong University, Shanghai 200240, People's Republic of China

<sup>a</sup>cyl666@sjtu.edu.cn, <sup>b</sup>guilin\_lu@sjtu.edu.cn, <sup>c</sup>zhongsh@sjtu.edu.cn, <sup>d</sup>wzshen@sjtu.edu.cn

**Abstract.** In this study, we fabricated n-type bifacial solar cells by liquid phase deposited (LPD) SiO<sub>2</sub> films as surface passivation layers. We have found that the growth conditions of LPD SiO<sub>2</sub> films have great influence on the deposition rate of the LPD SiO<sub>2</sub> films. Besides, the surface passivation effects of LPD SiO<sub>2</sub> films on both p-type and n-type silicon wafers are enormously improved after annealing at a temperature higher than 700 °C. Finally, the optimized LPD SiO<sub>2</sub> films have been successfully applied to the n-type bifacial silicon solar cells as the surface passivation layers, achieving a conversion efficiency of 19.06% on a large size (156 mm×156 mm) solar cell.

**Keywords:** Solar cell, N-type, Passivation, SiO<sub>2</sub>, Liquid phase deposition

## **1 Introduction**

So far, many efforts have been devoted to make n-type silicon wafers into silicon solar cells [1, 2, 3], due to the fact that n-type silicon wafer is superior to p-type silicon wafer in many aspects, such as minority carrier lifetime, metal contaminant tolerance [4] and light-induced degradation [5]. The n-Pasha cell from ECN is a typical structure of n-type bifacial solar cell [6]. For the bifacial solar cells, the passivation quality of the highly-doped boron emitter and phosphorus back surface field has a great influence on the final cell performance. Currently, one of the most widely used passivation techniques for n-type bifacial solar cell production is thermally-grown SiO<sub>2</sub> capped with SiN<sub>x</sub> [2, 3]. Though its surface passivation effect is excellent, it requires expensive equipment, high growth temperature and a long process step. In consideration of the cost-effectiveness, liquid phase deposited (LPD) SiO<sub>2</sub> film [7-10] with high qualities may provide a good solution, which is also compatible with the present solar cell mass production. Yuan *et al.*, [9] have first tried to use LPD SiO<sub>2</sub> film as the passivation layer of black silicon solar cells and acquired a conversion efficiency of 16.4%, showing the promising application of LPD SiO<sub>2</sub> film in silicon solar cells. He *et al.*, [10] have also applied LPD SiO<sub>2</sub> passivation layer to polycrystalline silicon solar cells, but the passivation effect and the final conversion efficiency (5.61%) are not satisfying.

---

\* Corresponding author: wzshen@sjtu.edu.cn

In this work, we have investigated the influence of  $H_2SiF_6$  concentration and deposition time on the deposition rate of LPD  $SiO_2$  film, as well as the effect of annealing temperature on the surface passivation quality of LPD  $SiO_2$  film on the silicon wafers. It is exciting that we successfully applied the optimized LPD  $SiO_2$  films to the n-type bifacial silicon solar cells as surface passivation layers, achieving a conversion efficiency of 19.06%.

## 2 Experiments

LPD  $SiO_2$  films passivated n-type bifacial silicon solar cells

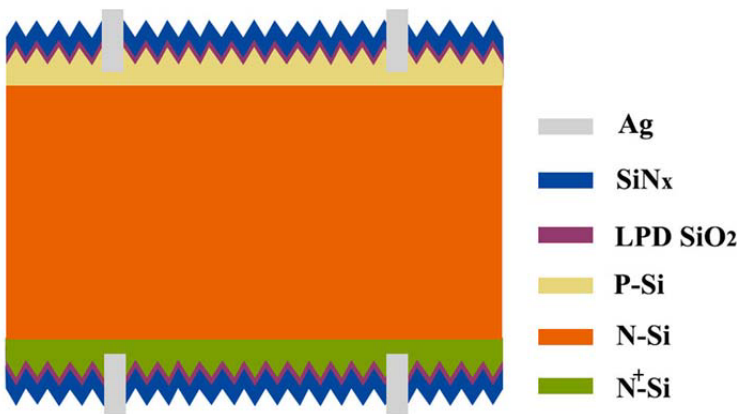


**Fig. 1** Schematic diagram of n-type bifacial silicon solar cell passivated by LPD  $SiO_2$  films.

For the fabrication of silicon solar cells, the crystalline silicon is Czochralski (Cz) N-type silicon with a resistivity of  $1\text{--}6 \Omega\cdot cm$ , a thickness of  $180 \mu m$  and an area of about  $238.95 \text{ cm}^2$ . Fig.1 shows the schematic diagram of n-type bifacial silicon solar cell. After the removal of damage layer, double-sided texturization, boron-doping for the front surface, removal of borosilicate glass, phosphorus implant for the back surface and activation of the implanted phosphorus by annealing, the silicon wafers were dipped in the dilute HF solution to remove the native oxide layers and then immersed into the silica-supersaturated  $H_2SiF_6$  solution to grow the LPD  $SiO_2$  films on both sides of the silicon wafers. The deposition processing of  $SiO_2$  is based on the hydrolysis reaction of silica-supersaturated hydrofluosilicic ( $H_2SiF_6$ ) acid, written as Eq. 1



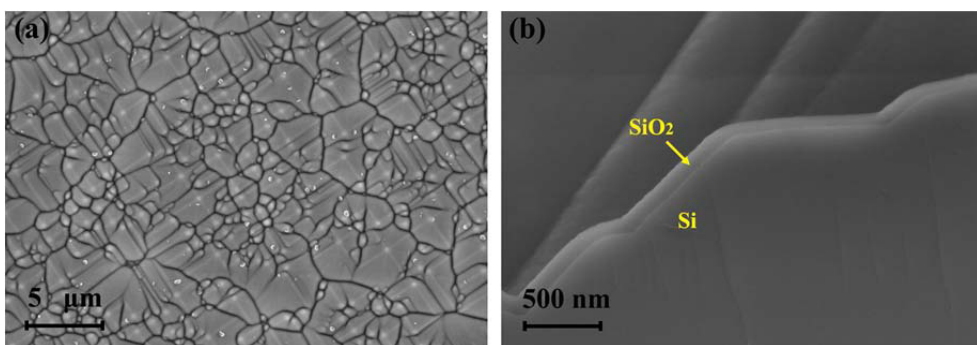
The specific method to prepare the growth solution (silica-supersaturated  $H_2SiF_6$ ) of LPD  $SiO_2$  films can be seen in reference [11]. Here, we chose the deposition temperature of  $50^\circ C$ , the  $H_2SiF_6$  concentration of  $1.5M$  and deposition time of 10 minutes to grow LPD  $SiO_2$  films for n-type bifacial silicon solar cell as its surface passivation films. Then the wafers were annealed in a muffle furnace at the annealing temperature of  $800^\circ C$  for 5 minutes to activate the passivation effect of LPD  $SiO_2$  films. Followed by depositing  $SiN_x$

antireflection layers on both sides, the electrodes were fabricated on the front and back sides by screen printing and co-fired technique.

## 2.1 Characterization

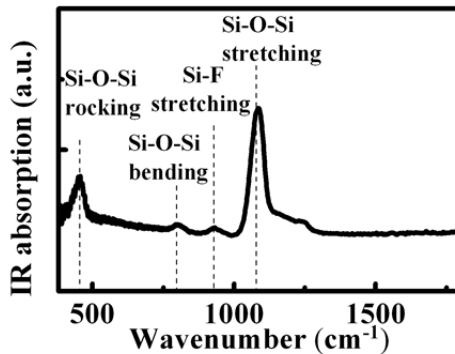
The effective minority carrier lifetime ( $\tau$ ) of the Si wafers symmetrically passivated by the LPD  $\text{SiO}_2$  films was measured by Semilab WT-1200A lifetime tester. The Thermolyne muffle furnace was used to study the impact of post-annealing on the surface passivation effect of the LPD  $\text{SiO}_2$  films. The surface morphologies of the LPD  $\text{SiO}_2$  films were observed by scanning electron microscope (SEM). Infrared absorption spectra were measured by Vertex 70 Fourier transform infrared (FTIR) spectrometer. The thicknesses of the LPD  $\text{SiO}_2$  films were determined by se800pv spectroscopic ellipsometry. The current ( $I$ )-voltage ( $V$ ) tester was used to measure the electrical performances of the LPD  $\text{SiO}_2$  film passivated n-type bifacial solar cells under AM 1.5 spectrum at the temperature of 25 °C.

## 3 Results and Discussion



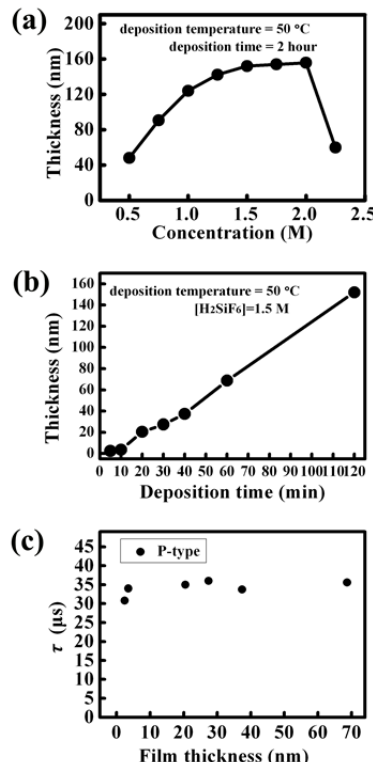
**Fig. 2(a)** Top view and (b) cross-sectional SEM images of the LPD  $\text{SiO}_2$  film grown on the pyramid structure textured silicon substrate.

For the morphological observation, we chose the films grown at 50 °C for two hours with 1.0 M  $\text{H}_2\text{SiF}_6$  without loss of generality. Fig. 2(a) and (b) respectively show the top-view and cross-sectional SEM images of LPD  $\text{SiO}_2$  film grown on the pyramid structure textured silicon surface that is the real surface condition of industrial silicon solar cells. As shown in Fig. 2(a) and (b), the high-coverage LPD  $\text{SiO}_2$  film is uniformly and densely deposited on the pyramid textures of silicon substrate.



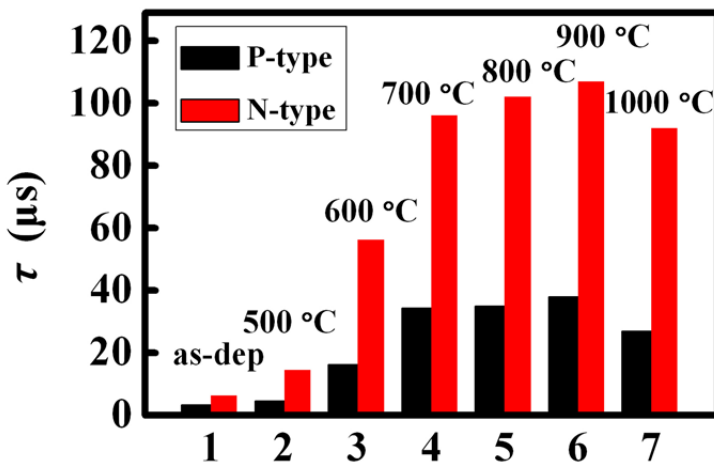
**Fig. 3** The FTIR spectrum of the as-deposited  $\text{SiO}_2$  film from 350 to 1800  $\text{cm}^{-1}$ .

Fig. 3 exhibits the FTIR spectra of the above sample. The infrared absorption characterized peaks located at 457  $\text{cm}^{-1}$ , 800  $\text{cm}^{-1}$  and 1085  $\text{cm}^{-1}$  correspond to Si-O-Si rocking vibration mode, Si-O-Si bending vibration mode and Si-O-Si stretching vibration mode, respectively [12,13]. The absorption peak at 931  $\text{cm}^{-1}$  is largely attributed to Si-F stretching vibration mode [12,13]. No other vibration signals of impurities such as carbon are detected by FTIR spectrometer, verifying the as-deposited LPD  $\text{SiO}_2$  is F-doped  $\text{SiO}_2$  with a pure chemical composition.



**Fig. 4** (a) Dependence of the thickness of the as-deposited LPD  $\text{SiO}_2$  film on  $\text{H}_2\text{SiF}_6$  concentration. (b) Dependence of the thickness of the as-deposited LPD  $\text{SiO}_2$  film on the deposition time. (c) Dependence of the  $\tau$  of post-annealed lifetime samples on the thickness of LPD  $\text{SiO}_2$  film.

By keeping other growth parameters unchanged, we have also investigated the effect of concentration of  $H_2SiF_6$  and the growth time on the thickness of LPD  $SiO_2$  film, respectively. As shown in Fig. 4(a), the thickness of the  $SiO_2$  film firstly increases with  $H_2SiF_6$  concentration from 0.5 up to 1.5 M, suggesting the increased deposition rate in the concentration range. This is because that the reversible reaction is promoted to the right side with increased  $H_2SiF_6$  concentration, thus the precipitation of  $SiO_2$  can be encouraged (see Eq. 1). Then the thickness of the  $SiO_2$  film keeps around 150 nm under  $H_2SiF_6$  concentrations of 1.5 to 2.0 M, achieving the maximum deposition rate of 75 nm/hour. However, the film thickness decreases dramatically when the  $H_2SiF_6$  concentration is increased to 2.25 M, which is ascribed to the insufficiency of  $H_2O$  (as a reactant) at an excessively high  $H_2SiF_6$  concentration. Considering the tradeoff between the growth rate and material cost, the  $H_2SiF_6$  concentration of 1.5 M is the optimal growth condition. Fig. 4(b) shows the dependence of the thickness of LPD  $SiO_2$  film on the deposition time. As can be seen in Fig. 4(b), the thickness of the LPD  $SiO_2$  film increases nonlinearly with the increased deposition time, and deposition rate of LPD  $SiO_2$  film is slower at the initial stage less than 10 minutes. This is because that incubation process of  $SiO_2$  precipitate on the substrates is inevitable. After this process, the growth rate of LPD  $SiO_2$  film remains almost a constant. To observe the impact of the thickness of LPD  $SiO_2$  film on surface passivation quality, the p-type silicon wafers (lifetime samples) are symmetrically passivated by the LPD  $SiO_2$  films, which are grown with 1.5 M  $H_2SiF_6$  concentration at deposition temperature of 50 °C for different deposition time (namely forming the  $SiO_2$  films with different thickness). The surface passivation effect of the LPD  $SiO_2$  films has been determined by the lifetime tester. Fig. 4(c) shows the  $\tau$  of these lifetime samples after annealed at the optimal annealing temperature (seen in Fig. 5). As can be seen in Fig. 4(c), the thickness of the LPD  $SiO_2$  film has little influence on  $\tau$  of lifetime samples, even the LPD  $SiO_2$  film with the thickness of 2.5 nm has a good surface passivation performance on the silicon wafer.



**Fig. 5** Histogram of  $\tau$  of the as-deposited and post-annealed lifetime samples.

To systematically investigate the effect of the annealing temperature on the passivation effect of LPD  $SiO_2$  film on the silicon wafers, both the p-type and n-type silicon wafers are symmetrically passivated by LPD  $SiO_2$  films and annealed at different temperatures for

5minutes in muffle furnace. The growth condition of LPD SiO<sub>2</sub> films keeps a constant with H<sub>2</sub>SiF<sub>6</sub> concentration of 1.5 M, growth temperature of 50 °C and growth time of 2 hours. As the data shown in Fig. 5, the  $\tau$  of p-type and n-type sample with the as-deposited LPD SiO<sub>2</sub> films are 3.18 and 6.18  $\mu$ s, respectively. These values are comparable to that of naked Si wafers, indicating a rather poor surface passivation quality of the as-deposited SiO<sub>2</sub> film. However, the surface passivation effect of the LPD SiO<sub>2</sub> film can be significantly enhanced by the annealing process. The  $\tau$  of p-type and n-type samples both gradually increases with the increased annealing temperature from 500 to 700 °C, then keeps around 35  $\mu$ s for p-type samples and 100  $\mu$ s for n-type samples at annealing temperature of 700 to 900 °C, achieving the optimal surface passivation effect of LPD SiO<sub>2</sub> films. This improved  $\tau$  can be attributed to the reconstruction of the Si/SiO<sub>2</sub> interface, which makes the dangling bonds on surface of silicon wafer effectively passivated. However, the passivation effect of the SiO<sub>2</sub> film on both the p-type and n-type silicon wafers begins to decline at a higher annealing temperature of 1000 °C. The effective surface recombination velocity ( $S_{eff}$ ) of p-type and n-type sample after annealed at the optimal annealing temperature are 260 and 110 cm/s, respectively, which are comparable to that of float zone(FZ) silicon wafers passivated by high-rate plasma-deposited SiO<sub>2</sub> films [14] , indicating that the importance of both the chemical passivation and the field-effect passivation in the passivation mechanism.

**TABLE 1 THE CELL PERFORMANCE OF LPD SiO<sub>2</sub> FILM PASSIVATED N-TYPE BIFACIAL SILICON SOLAR CELL.**

$V_{oc}$ [mV]	$J_{sc}$ [mA/cm <sup>2</sup> ]	FF	EFF	$R_s$ [ $\Omega$ cm <sup>2</sup> ]
632	39.58	76.52%	19.06%	4.33

We have successfully introduced the LPD SiO<sub>2</sub> film to the industrial fabrication of N-type bifacial solar cell. It should be noted that the thickness of LPD SiO<sub>2</sub> film has been controlled at around 3 nm to promise the entire puncture of Ag paste through the LPD SiO<sub>2</sub> film during the co-fired process. In the study, we fabricated three batches of LPD SiO<sub>2</sub> film passivated n-type bifacial silicon solar cells, and the electrical performance of them were very similar. As a result, we chose one set of data to be shown in Table 1. The conversion efficiency (EFF) achieves 19.06% with an open circuit voltage ( $V_{oc}$ ) of 632 mV, a short circuit current density of 39.58 ( $J_{sc}$ ) mA/cm<sup>2</sup>, demonstrating the successful application of the LPD SiO<sub>2</sub> film in n-type bifacial silicon solar cells. A good fill factor (FF) of 76.52% and a series resistance ( $R_s$ ) of 4.33  $\Omega$ cm<sup>2</sup> indicate a good electrode contact. Besides, the surface of the solar cells without obvious chromatic aberration reveals that our LPD SiO<sub>2</sub> film is perfectly uniform. We can anticipate that the thicker LPD SiO<sub>2</sub> film simultaneously play the roles of antireflection and passivation layers with using laser to open windows for electrode contact, the advantage of the LPD technique will be more obvious.

## 4 Summary

The SiO<sub>2</sub> films with high purity, uniformity and perfect-coverage have been successfully grown by a liquid phase deposition technique. We found out that the growth parameters have great influence on the deposition rate of LPD SiO<sub>2</sub> film. The passivation effect of as-deposited LPD SiO<sub>2</sub> films on silicon wafers is poor but can be dramatically improved by annealed at temperature higher than 700 °C. Finally, we have successfully applied the LPD SiO<sub>2</sub> films to n-type bifacial silicon solar cells as the surface passivation layers and realized an efficiency of 19.06% on a large size solar cell (156 mm×156 mm). We believe that the cost-effective passivation technique presented in this work opens a new opportunity for high-efficiency silicon solar cells.

## Acknowledgements

This work was supported by the Natural Science Foundation of China (61234005 and 11474201), and Shanghai Municipal Project (14DZ1201000).

## References

1. J. Benick, B. Hoex, M.C.M. van de Sanden, W.M.M. Kessels, O. Schultz, and S.W. Glunz, High efficiency n-type Si solar cells on Al<sub>2</sub>O<sub>3</sub>-passivated boron emitters, *Applied Physics Letters* 92 (2008) 253504.
2. L. Tous, M. Aleman, R. Russell, E. Cornagliotti, P. Choulat, A. Uruena, S. Singh, J. John, F. Duerinckx, J. Poortmans and R. Mertens, Evaluation of advanced p-PERL and n-PERT large area silicon solar cells with 20.5% energy conversion efficiencies, *Progress in Photovoltaics: Research and Applications* 23 (2015) 660-670.
3. A. Lanterne, S. Gall, Y. Veschetti, R. Cabal, M. Coig, F. Milési, A. Tauzin, High efficiency fully implanted and co-annealed bifacial n-type solar cells, *Energy Procedia* 38 (2013) 283-288.
4. D. Macdonald, L.J. Geerligs, Recombination activity of interstitial iron and other transition metal point defects in p- and n-type crystalline silicon, *Applied Physics Letters* 85 (2004) 4061-4063.
5. K. Bothe, J. Schmidt, Electronically activated boron-oxygen-related recombination centers in crystalline silicon, *Journal of Applied Physics* 99 (2006) 013701.
6. A.R. Burgers, L.J. Geerligs, A.J. Carr, A. Gutjahr, D.S. Saynova, J.F. Xiong, G.F. Li, Z. Xu, H.F. Wang, H. An, Z.Y. Hu, P.R. Venema, A.H.G. Vlooswijk, 19.5% efficient n-type Si solar cells made in production, 26th European Photovoltaic Solar Energy Conference and Exhibition, 2011 pp. 1144-1147.
7. H. Nagayama, H. Honda, H. Kawahara, A new process for silica coating, *Journal of the Electrochemical Society* 135 (1988) 2013-2016.
8. C.J. Huang, Quality optimization of liquid phase deposition SiO<sub>2</sub> films on silicon, *Japanese Journal of Applied Physics* 41 (2002) 4622-4625.
9. H.C. Yuan, J.H. Oh, Y. C. Zhang, O. A. Kuznetsov, D. J. Flood, H.M. Branz, Antireflection and SiO<sub>2</sub> surface passivation by liquid-phase chemistry for efficient black silicon solar cells, 38th IEEE Photovoltaic Specialists Conference, 2012, pp. 686-689.
10. J. He, Y.C. Ke, G.L. Zhang, Q.C. Deng, H. Shen, S.C. Lu, M.R. Qin, X. Wang, C.L. Zeng, Liquid phase deposited SiO<sub>2</sub> on multi-crystalline silicon, *Polymers Research Journal* 9 (2015) 57-65.
11. B.C. Hsu, W.C. Hua, C.R. Shie, K.F. Chen, C.W. Liu, Growth and electrical characteristics of liquid-phase deposited SiO<sub>2</sub> on Ge, *Electrochemical and Solid-State Letters* 6 (2003) F9-F11.
12. C.J. Huang, J.-R. Chen, S.P. Huang, Silicon dioxide passivation of gallium arsenide by liquid phase deposition, *Materials Chemistry and Physics* 70 (2001) 78-83.
13. H.R. Wu, K.W. Lee, T.B. Nian, D.W. Chou, J.J. Huang Wu, Y.H. Wang, M.P. Houng, P.W. Sze, Y.K. Su, S.J. Chang, C.H. Ho, C.I. Chiang, Y.T. Chern, F.S. Juang, T.C. Wen, W.I. Lee, J.I. Chyi, Liquid phase deposited SiO<sub>2</sub> on GaN, *Materials Chemistry and Physics* 80 (2003) 329-333.
14. B. Heox, F.J.J. Peeters, M. Creatore, M. A. Blauw, W.M.M. Kessels, M.C.M. van de Sanden, High-rate plasma-deposited SiO<sub>2</sub> films for surface passivation of crystalline silicon, *Journal of Vacuum Science and Technology A* 24 (2006) 1823-1830.